Measurement of HO_2NO_2 in the Upper Troposphere during ICARRT-INTEX-NA 2004

[1]L.G. Huey, [1]S. Kim, [1]R.E. Stickel, [1]D.J. Tanner, [2]J. H. Crawford, [2]J. R. Olson, [2]G. Chen, [3]W. H. Brune, [3]X. Ren, [3]R. Lesher, [4]P. J. Wooldridge, [4]T. H. Bertram, [4]A. Perring, [4]R. C. Cohen, B., [5,*]B. Lefer, [5]R. E. Shetter, [2]M. Avery, [2]G. Diskin, and [1]I. Sokolik

[1]School of Earth and Atmospheric Sciences, Georgia Institute of Technology

Atlanta, GA, 30332, USA

[2]NASA Langley Research Center, Hampton, VA 23681, USA

[3]Department of Meteorology, Penn State University, University Park, PA 16802, USA

[4]Department of Chemistry and Department of Earth and Planetary Science, University of California Berkeley, Berkeley, CA, 94720, USA

[5]National Center for Atmospheric Research, Boulder, CO 80305, USA

[*]present: Department of Geosciences, University of Houston, Houston, TX 77204, USA

The first direct *in situ* measurements of HO_2NO_2 in the upper troposphere were performed from the NASA DC-8 during ICARTT-INTEX-NA 2004 with a chemical ionization mass spectrometer (CIMS). These measurements provide an independent diagnostic of HO_x chemistry in the free troposphere and complement direct observations of HO_x, due to its dual dependency on HO_x and NO_x. On average, the highest HO_2NO_2 mixing ratio of 76 pptv (median = 77pptv, σ = 39 pptv) was observed at altitudes of 8-9 km. HO_2NO_2 levels were lower above and below this altitude. Simple steady state calculations of HO_2NO_2, constrained by measurements of HO_x, NO_x and J values, are in good

agreement (slope = 0.90, R^2 = 0.60 z = 5.5-7.5 km) with measurements in the mid troposphere where thermal decomposition is the major loss process. Above 8 km these calculations are in poor agreement with observed values (R^2= 0.20) and are typically larger by a factor of 2.4. Conversely, steady state calculations using model derived HO_x show reasonable agreement with the observed HO_2NO_2 in both the mid troposphere (slope = 0.96, intercept =7.0, R^2 = 0.63) and upper troposphere (slope = 0.80, intercept = 32.2, R^2 = 0.58). Potential reasons for the model/measurement discrepancies are investigated.

1. Introduction

Pernitric acid (HO_2NO_2) is formed in the atmosphere by an association reaction that couples the HO_x and NO_x families [*Niki et al*., 1977]:

$$HO_2 + NO_2 + M \leftrightarrow HO_2NO_2 + M \qquad R1, R\text{-}1$$

The thermal decomposition of HO_2NO_2 R-1 is a strong function of temperature with the lifetime for this process varying between approximately 20 seconds and 8 hours over the altitude range of 0 to 8 km. Consequently, at lower and mid latitudes, HO_2NO_2 is only expected to build up to significant concentrations in the upper troposphere; where photolysis and reaction with OH are expected to be the dominant loss processes.

$$HO_2NO_2 + h\nu \rightarrow \text{Products} \qquad R2$$

$$OH + HO_2NO_2 \rightarrow H_2O + NO_2 + O_2 \qquad R3$$

The potential impact of HO_2NO_2 on upper tropospheric photochemistry (z = 8-12 km) has been discussed by several investigators [*Brune et al.* 1999; *Wennberg et al.* 1999; *Faloona et al.* 2000]. In particular, *Jaeglé et al*. [2000] noted the importance of HO_2NO_2 as a HO_x sink at intermediate levels of NO_x (100 - 500 pptv) via R3. However, these studies were unconstrained by observations of HO_2NO_2. The only previous direct measurements of HO_2NO_2 are in the South Pole boundary layer during Austral Summer 2000 and 2003

[*Slusher et al.*, 2002; *Sjostedt et al,* 2004]. These results demonstrated the HO_2NO_2 was present in significant levels (on average 25 pptv in 2000; 42 pptv in 2003) and could be the dominant sink for HO_x via deposition to the snowpack and R3. The only *in situ* airborne HO_2NO_2 data was obtained during the TOPSE campaign from the NCAR C-130 at latitudes of 0 to 7 km. *Murphy et al*. [2003] derived levels of $HO_2NO_2 + CH_3ONO_2$ from their sum of peroxy nitrates channel (ΔPN) by subtracting independent measurements of peroxy acyl nitrates (PANs). Analysis of this data demonstrated the importance of the overtone photolysis channels as a loss mechanism for HO_2NO_2 [*Roehl et al*, 2002; *Wennberg et al*, 1999]. Observations of pernitric acid by remote sensing have been reported but are confined to the stratosphere [*Rinsland et al*., 1996; *Sen et al.*, 1998].

Here we present the first direct *in situ* observations of HO_2NO_2 in the upper troposphere. These measurements were performed in the summer of 2004 with a chemical ionization mass spectrometer from the NASA DC-8 during the Intercontinental Chemical Transport Experiment-North America (INTEX-NA) field experiment. The INTEX-NA study sought to characterize and investigate the transport and transformation of both aerosol and gas-phase species over large spatial scales and altitude ranges. Flights were based out of California, Illinois, and New Hampshire. The sampling domain included much of the

U.S., parts of Canada, and areas off the eastern and western coasts of North America. A detailed description of the DC-8 payload and the INTEX-NA campaign is presented by *Singh et al*., [this issue]. In this work the our understanding of the chemistry of HO_2NO_2 over the altitude range 4-12 km is investigated by comparison of observations with highly constrained steady state calculations and photochemical models

2. Methods

2.1 Instrumentation

The instrument used to measure HO_2NO_2 and SO_2 from the NASA DC-8 during INTEX-NA is nearly identical to that described by *Slusher et al*. [2004]. The instrument comprises an inlet, a flow tube ion molecule reactor, a collisional dissociation chamber (CDC), an octopole ion guide and a quadrupole mass spectrometer as shown in Figure 1. Briefly, SF_6^- ion chemistry is utilized to selectively ionize HO_2NO_2 and SO_2 (R4 and R5) in the CIMS [*Slusher et al*., 2001; *Huey et al*., 1995; *Huey et al*., 2004].

$$SF_6^- + HO_2NO_2 \rightarrow NO_4^-(HF) + SF_5 \quad R4$$

$$SF_6^- + SO_2 \rightarrow F_2SO_2^- + SF_4 \quad R5$$

Air was delivered to the CIMS through an all perfluoroalkoxy Teflon inlet (i.d.= 0.95 cm, length= 80 cm) maintained at a constant temperature of 298 K. A flow of more than 5 slpm

was maintained in the inlet to minimize both the gas residence time (t<0.57sec) and wall interaction. The sampled air was periodically scrubbed of both HO_2NO_2 and SO_2 with an activated carbon filter. The sensitivity of the instrument to SO_2 was continuously monitored by the addition of isotopically labeled calibration gas (850ppbv ± 9.2%) [e.g. *Bandy et al*., 1993]. A typical example of the raw CIMS data is shown in Figure 2. The sensitivity of HO_2NO_2 relative to SO_2 was assessed post mission by a series of laboratory tests over the pressure and humidity conditions encountered on the DC-8. These tests demonstrated that the relative sensitivity of the instrument of HO_2NO_2 to SO_2 was nearly identical to the ratio of the rate constants for reactions R4 and R5 [*Slusher et al.*2001]. The estimated uncertainty for HO_2NO_2 levels well above detection limit was typically 30% with a detection limit of less than 5 pptv for a one minute integration at altitudes greater than 3 km .The methods used to obtain HO_x, NO_2, and J values during INTEX-NA have been described in detail elsewhere [Brune et al; Bertram et al; *Shetter and Müller* 1999].

2.2 Calculations

HO_2NO_2 levels were estimated, assuming steady state, from the following equation.

$$[HO_2NO_2]_{SS} = \frac{k_1[HO_2][NO_2]}{J_3 + k_{-1} + k_2[OH]} \qquad (1)$$

The rate constants for these calculations are taken from *Christensen et al*., [2004] for k_1, *Sander et al.* [2003] for k_{-1} and *Jiménez et al*., [2004] for k_3. The NO_2 mixing ratios and the photolysis rate in the ultraviolet region were constrained by observations. Actinic fluxes in the near infrared were not measured during this campaign leaving the overtone photolysis rate unconstrained. For this reason, the overtone photolysis rate was estimated to be 10^{-5} sec^{-1} [*Murphy et al*. 2003; *Roehl et al.,* 2002; *Wennberg et al,* 1999]. Pernitric levels were calculated using both observed ($[HO_2NO_2]_{ss,obs}$) and model predicted ($[HO_2NO_2]_{ss,mod}$) levels of OH and HO_2. Model predicted HO_x levels were obtained from the NASA-Langley photochemical box model which was highly constrained to observations of photolyis rates and the concentrations of long lived species (e.g. NO_2, O_3, CO, etc.) [*Olson et al.,* 2004; *Crawford et al*., 1999].

Time dependent model calculations are also performed to assess the deviation of HO_2NO_2 from steady state for typical upper tropospheric condition where its lifetime is of the order of five hours (Figure 3). This method assumed an initial injection of NO_x into the upper troposphere and followed its temporal evolution and oxidation over the course of several days in one minute time steps. Short lived species such as radicals were predicted

using the steady state assumption and the chemical scheme of *Faloona et al* [2000]. Longer lived species such as CO were held at median observed values. The chemical species and how they were treated in the model are listed in Table 1. All photolysis rates were calculated with the TUV 4.1 model (http://cprm.acd.ucar.edu/Models/TUV/) and rate constants were taken from the JPL evaluation version 14 [*Sanders et al.,* 2003].

3. Result and Analysis

All reported data and analyses are based on a one minute average merged data set (ftp://ftp-air.larc.nasa.gov/pub/INTEXA/DC8_AIRCRAFT/). The median observed HO_2NO_2 altitude profile for the INTEX-NA mission is presented in Figure 4 and the statistics of the vertical distribution are reported in Table 1. Median steady state calculations of HO_2NO_2 based on both observed and model predicted HO_x are also graphed in Figure 4. The observed HO_2NO_2 mixing ratio profile shows a maximum of ~75 pptv between 8 and 9 km. Pernitric acid mixing decrease below this altitude as expected due to enhance thermal dissociation rates. Above 10 km levels decrease primarily due to a weakening of the source strength. The mean concentration of pernitric acid in the upper troposphere (8 ~ 12 km) is 67±37 pptv (2467 data points, 1σ). This value is in reasonable

agreement with constrained calculations of mean HO_2NO_2 values of 55 ± 30 pptv from the SONEX campaign, a previous DC-8 mission [*Talbot et al*., 1999]. However, it should be noted that SONEX took place north of INTEX in the Fall (October through November, 1997) [*Singh et al.,* 1999].

In the mid troposphere (4km - 8km) both of the calculated profiles are in reasonable agreement with observations (Figure 4). This is more clearly illustrated in Figure 5 which presents scatter plots of the steady state calculations versus observations. The calculations base on observed HO_x (Figure 5a, R^2= 0.60, slope = 0.90, intercept = 0.4 pptv) and on model predicted HO_x (Figure 5b, R^2= 0.63, slope = 0.96 intercept = 7.0 pptv) are both well correlated to the observations. The median ratios for the calculations relative to the observations are 0.8 for observed HO_x and 1.1 for model predicted HO_x. This level of agreement is well within the 30% error bar of the HO_2NO_2 measurement alone. These results indicate that our understanding of the chemistry of HO_2NO_2 is very good in this region, where thermal decomposition dominates the lifetime (Figure 3). Very similar results were also derived using k_{-1} from the recent work of *Gierczak* et al., [2005]. Correlations between calculations and observations were essentially identical with calculated values rising by a factor of 1.5.

In the upper troposphere (8-12 km) the agreement between the steady state calculations and observations is not as good as at lower altitudes. The HO_2NO_2 calculations based on model predicted HO_x are still highly correlated with the observations (Figure 6b, R^2=0.58, slope = 0.80, intercept = 32.2 pptv) but with a significant offset that yields a median ratio of calculated to observed of 1.3. Conversely, the correlation between HO_2NO_2 calculations based on observed HO_x and observations is significantly weaker (Figure 6a , R^2=0.20, slope = 1.38, intercept = 72.4 pptv) with a median ratio of calculated to observed of 2.4. These results indicate that our ability to predict HO_2NO_2 with simple steady state models at higher altitudes, where its lifetime is longer and controlled by photochemical processes (Figure 3), is not as good as at low altitudes. There is also a clear discrepancy between upper tropospheric HO_x observations and predictions, with the pernitric observations more in accord with the photochemical model results.

At altitudes above 8 km the photochemical model over predicts OH by roughly a factor of two and under predicts HO_2 by roughly a factor of two relative to the observations [reference Ren et al.?]. This gives an even larger discrepancy between the measured and predicted HO_2 to OH ratio. At higher altitudes where thermal decomposition of pernitric is negligible the ratio of HO_2NO_2 to NO_2 would be expected to have a reasonable correlation

to the ratio of HO_2 to OH .This is evident from equation 1 for those conditions where reaction with OH (R3) is the dominant loss. For most conditions the HO_2NO_2 loss due to photolysis and reaction with OH are of similar magnitudes. However, the correlation between $[HO_2]/[OH]$ and $[HO_2NO_2]/[NO_2]$ should still be significant due to the dependence of OH levels on photolysis rates. A strong correlation ($R^2 = 0.7$) is observed between model predicted $[HO_2]/[OH]$ (Figure 7a) and observed $[HO_2NO_2]/[NO_2]$, however, the correlation decreases significantly with observed HO_x (Figure 7b, R^2=0.3).

A potential problem with the SF_6^- CIMS system for measurement of HO_2NO_2 is a positive interference due to high ozone levels [*Slusher et al*., 2001]. This potential effect was investigated during the INTEX mission by examining the relationship of observed HO_2NO_2 with O_3. Figure 8 plots observed HO_2NO_2 versus O_3 in the altitude range of 8.5 – 9.5 km (i.e. highest HO_2NO_2) for both periods of when the air was primarily of tropospheric (O_3<150 ppbv, H_2O>120ppmv) and stratospheric origin (O_3>200 ppbv, H_2O<100ppmv). There is a moderate correlation (R^2=0.33) between pernitric acid and ozone at lower ozone levels for the tropospheric air masses. At the higher ozone levels in the stratospherically influenced air masses there is essentially no correlation. This indicates that O_3 at levels of up to 250 ppbv don't give a significant interference to the HO_2NO_2

measurement. The correlation between ozone and HO_2NO_2 in the tropospheric air masses is likely due to ozone production via the reaction of HO_2 with NO which is closely related to pernitric formation (R1). This suggests that HO_2NO_2 in this altitude range may be a good marker for ozone production.

4. Discussion

At altitudes below 7.5 km there is good agreement between measurements of HO_x, NO_x, HO_2NO_2, and our understanding of photochemistry as embodied in the photochemical model predictions. The thermal decomposition rates derived from *Sander et al.* [2003] and *Gierzcak et al.* [2005] are both in reasonable agreement with the lower altitude observations. The slower decomposition rate derived from *Gierzcak et al*. [2005] does leads to over prediction of observed HO_2NO_2 by 30 to 50%. However, this agreement is within the combined error bars of the HO_x, NO_x and HO_2NO_2 measurements. These results indicate that the uncertainty in the HO_2NO_2 lifetime due to the thermal decomposition rate, k_{-1}, is less than a factor of two.

Above 8 km the observations of HO_x and HO_2NO_2 are less compatible with our understanding of photochemistry. The results indicate that HO_2NO_2 loss rates are

underestimated or that steady state calculations are problematic in this altitude range and the agreement between be model HO_x calculations and observed HO_2NO_2 is fortuitous. For this reason, we have investigated potential loss processes, reassessed our estimate of overtone photolysis rates, and performed time-dependent photochemical calculations to assess the magnitude of deviation from steady state.

Pernitric acid could be lost by heterogeneous loss or uptake in the upper troposphere on either background sulfate aerosol or cirrus clouds [*Li et al.*, 1996]. However, we found no evidence for a relationship between aerosol surface area densities and HO_2NO_2 levels indicating that reaction on sulfate aerosol is not an important loss process. Evaluating the impact of cirrus clouds on pernitric acid levels is more problematic due to their relatively short lifetime (~1 hour). There were a few flight legs during the campaign that the DC-8 sampled in cirrus as evidenced by detection of large particles (>20 μm dia.). There was no obvious diminishment of pernitric acid in these air masses but this data is limited and doesn't allow for a robust conclusion. For this reason, we think cirrus cloud processing of HO_2NO_2 is still an open question especially since pernitric acid has been shown to efficiently stick to ice at low temperatures [*Li et al.*, 1996].

Overtone photolysis rates of HO_2NO_2 were estimated by calculating actinic fluxes using the SBDART (Santa Barbara DISORT Atmospheric Tranfer) model and cross sections and quantum yields from *Roehl et al.* [2002]. Calculations of both direct and diffuse fluxes were performed for typical INTEX conditions listed in Table 3. Note that sand was chosen as the surface to maximize the infrared albedo. A total photolysis rate of 8 x 10^{-6} s^{-1} was calculated which compares favorably with the value of 8.3 x 10^{-6} s^{-1} derived by *Roehl et al.*,[2002] direct flux at the top of the atmosphere. These calculations support the estimated photolysis rate (10^{-5} s^{-1}) used in the steady state analysis. Although the dominant overtone photolysis band, $2v_1$, for HO_2NO_2 overlaps a water transition (*Rothman et al.*, 2005) which greatly attenuates the upward flux in this spectral range over clouds, snowpacks, and ocean. This indicates that the calculated photolysis rate is an upper limit and could be diminished by the presence of clouds. It is also worth noting that only one measurement [*Roehl et al.*,2002]of the quantum yields and cross section for the $2v_1$ band is available and should probably be confirmed.

The error in the HO_2NO_2 calculations was investigated by using a time-dependent photochemical model to estimate the deviation from steady state. Figure 9 shows a temporal plot of HO_2NO_2 at 9 km, for typical INTEX_NA conditions, calculated using

steady state and time-dependent methods. The time-dependent results are for the third day after a fresh injection of NO_x into the upper atmosphere reflecting the relatively fresh air-masses sampled during INTEX-NA [*Fuelberg et al.*, *Bertram et al.* in this issue]. The shaded area in Figure 9 is the typical flight time from 8am to 5pm. The largest difference is in the morning where the steady state model over predicts HO_2NO_2 by ~50%. The disagreement diminishes through the day until there is a slight underestimation by the steady state model in the late afternoon. On average the steady state model over predicts the time-dependent results by 12%. At higher altitudes the disagreement between steady state and time-dependent calculations is less as HO_2NO_2 doesn't undergo significant thermal decomposition through the night. Consequently, steady state methods seem to be valid for predicting HO_2NO_2 levels in the upper troposphere with less than a 50% inherent error bar.

Clearly, the measured HO_2NO_2 and HO_x are not consistent with our current understanding of photochemistry in the upper troposphere. A higher loss rate for pernitric acid would bring observations of HO_2NO_2 and HO_2 into better agreement. Figure 10a presents the vertical profile of the needed HO_2NO_2 first order rate constant for the additional loss needed to bring observed HO_2NO_2 and HO_x into accord. This additional loss rate generally increases with altitude with a maximum near 11 km. One potential

mechanism that could account for the additional loss is photolysis via weak electronic transitions as discussed by *Mathews et al.*, [2005]. Finally, we checked to see if the measured OH and the model predicted HO_2/OH ratio are consistent with the observed HO_2NO_2. This was done with a steady state analysis using observed OH and HO_2 derived from the predicted HO_x ratio. The median altitude profile for this data is shown in Figure 10b and shows excellent agreement with the observed profile. This data demonstrates that the observed HO_2NO_2 are primarily inconsistent with the observed HO_2 ratio but not the observed OH levels.

5. Summary

Our understanding of HO_2NO_2 in the free troposphere is examined with the first direct in-situ observations from INTEX-NA 2004. Photochemical models and observed HO_x levels can explain the HO_2NO_2 in the mid troposphere (4.5-8 km) where thermal decomposition is dominant. In the upper troposphere (8-12 km) there is a significant discrepancy between predicted and observed HO_x and the HO_2NO_2 observations are more consistent with the model results. This discrepancy could be diminished if there is an unidentified loss process for HO_2NO_2 whose magnitude increases with altitude. This

suggests that further laboratory studies of the chemistry of HO_2NO_2 may be warranted. These data also demonstrate the value of HO_2NO_2 observations as a valuable constraint on the radical cycling in the upper troposphere.

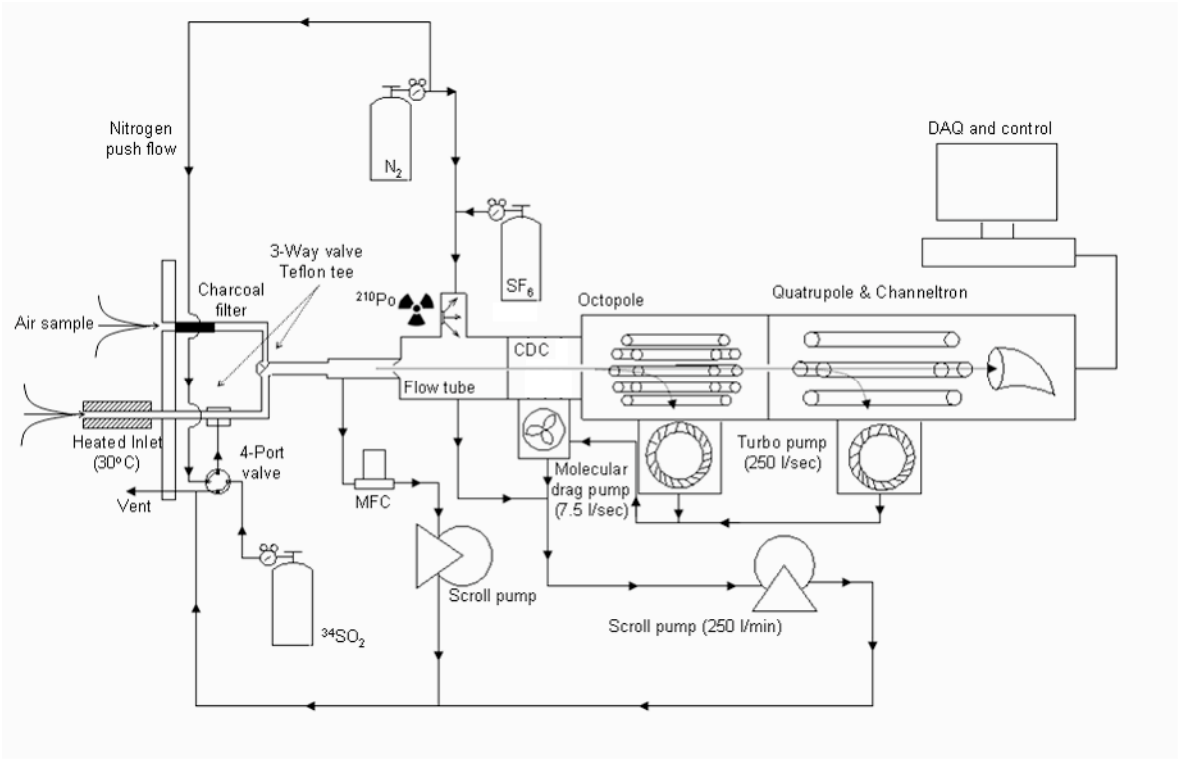

Figure 1. Diagram of CIMS system integrated

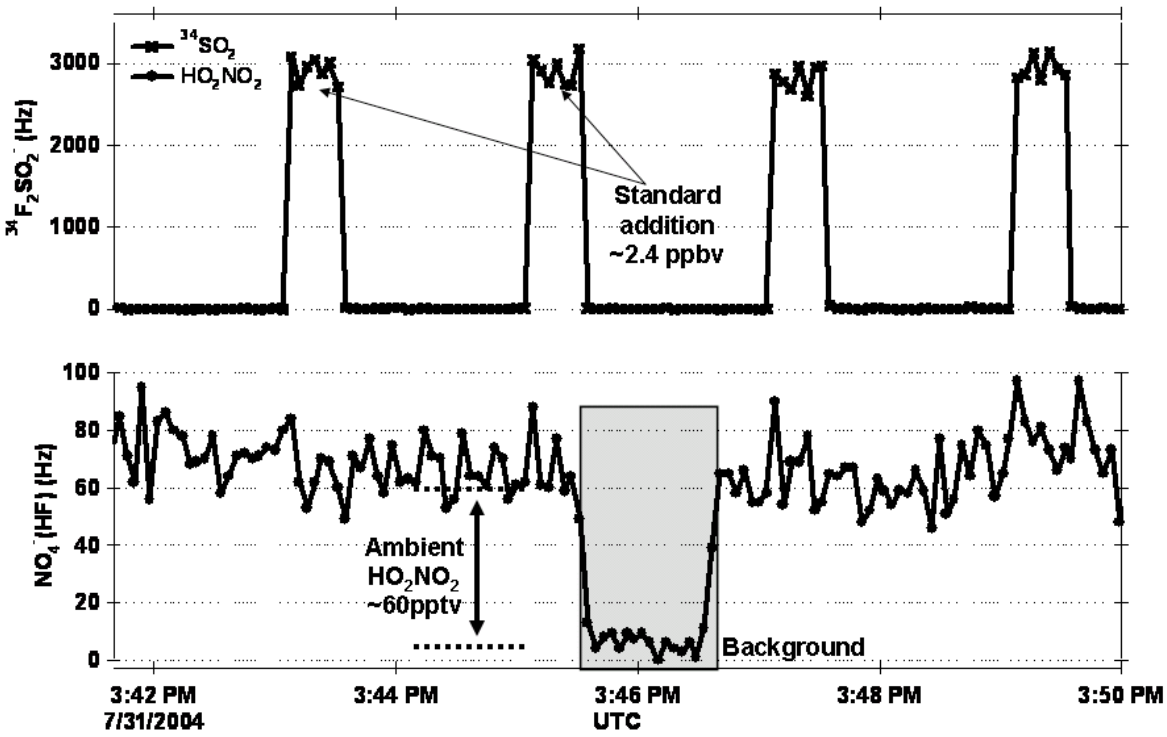

Figure 2 Raw ion signal obtained during flight. The upper panel is the $^{34}SO_2$ signal and illustrates the periodic calibration to the labeled standard. The lower panel shows variation of ambient signal HO_2NO_2 signal. The shaded area in the lower panel is a background measurement period.

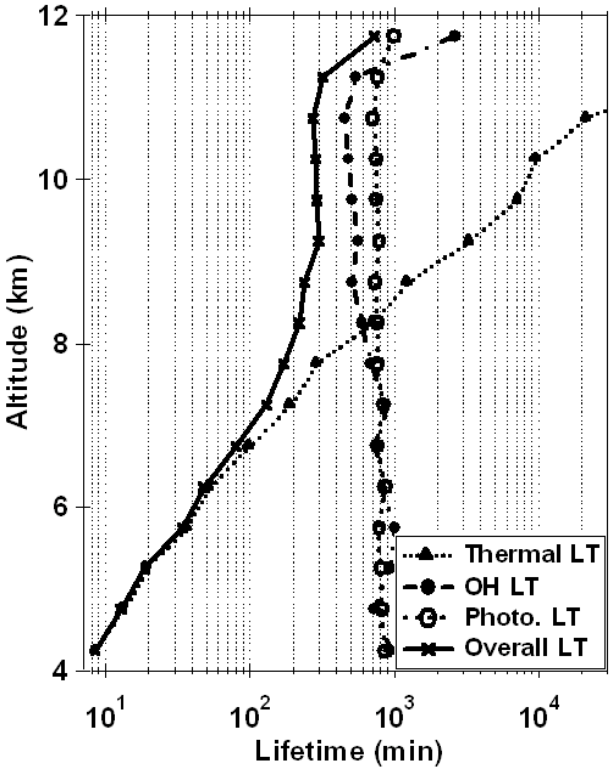

Figure 3. Vertical distribution of the total lifetime of HO_2NO_2 (x) and individual lifetimes with respect to thermal decomposition (triangles), photolysis (circles), and OH reaction (filled circles).

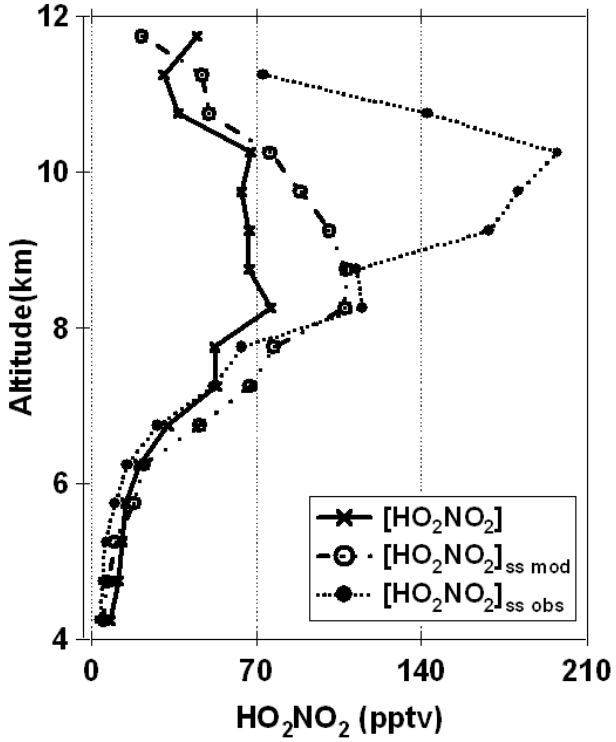

Figure 4. Vertical distribution of observed HO_2NO_2 (x) and predictions based on model predicted (open circles) and observed (filled circles) HO_x.

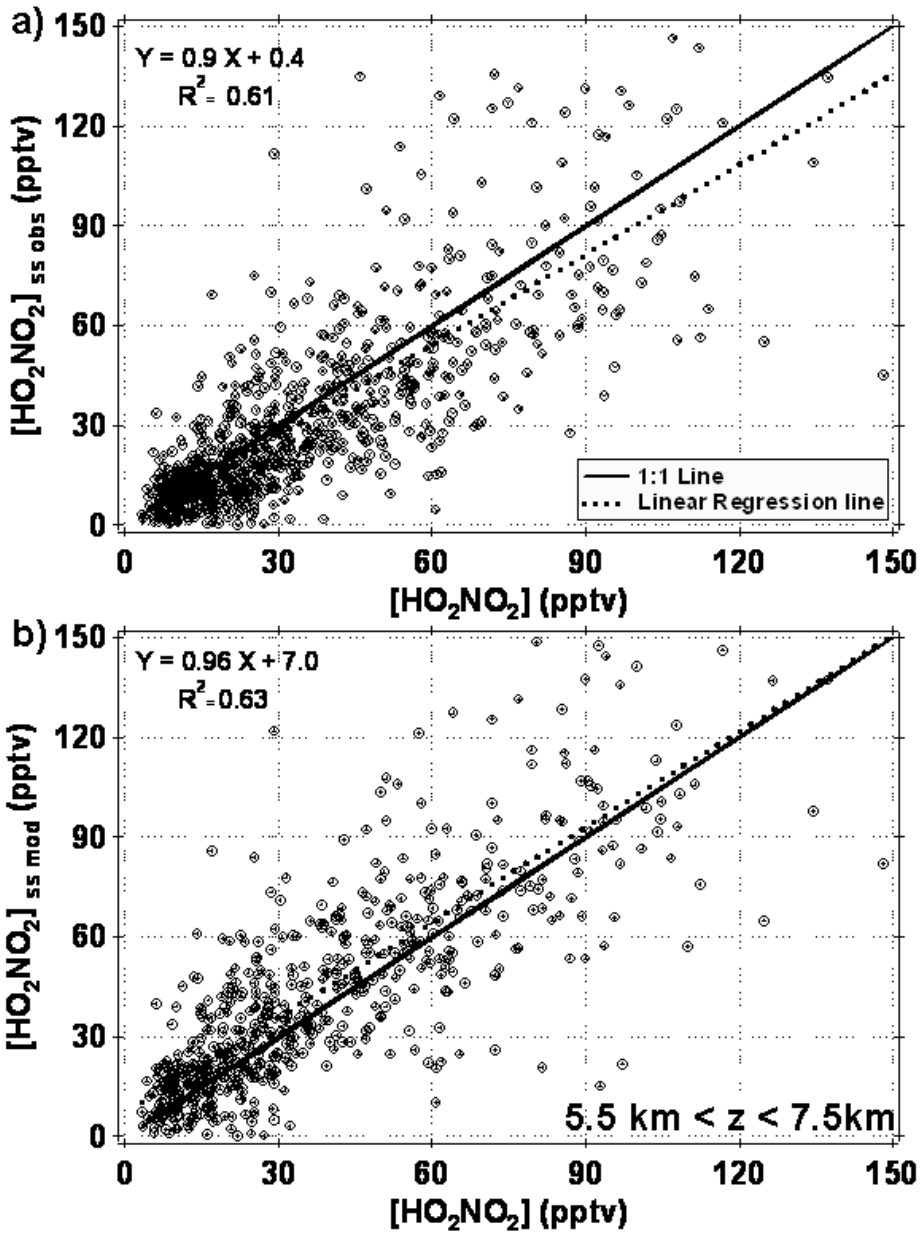

Figure 5. Scatters plots of mid troposphere (5.5-7.5km) HO_2NO_2 steady state calculations versus observed HO_2NO_2. The calculations are based on observed (upper panel) and model (lower panel) HO_x.

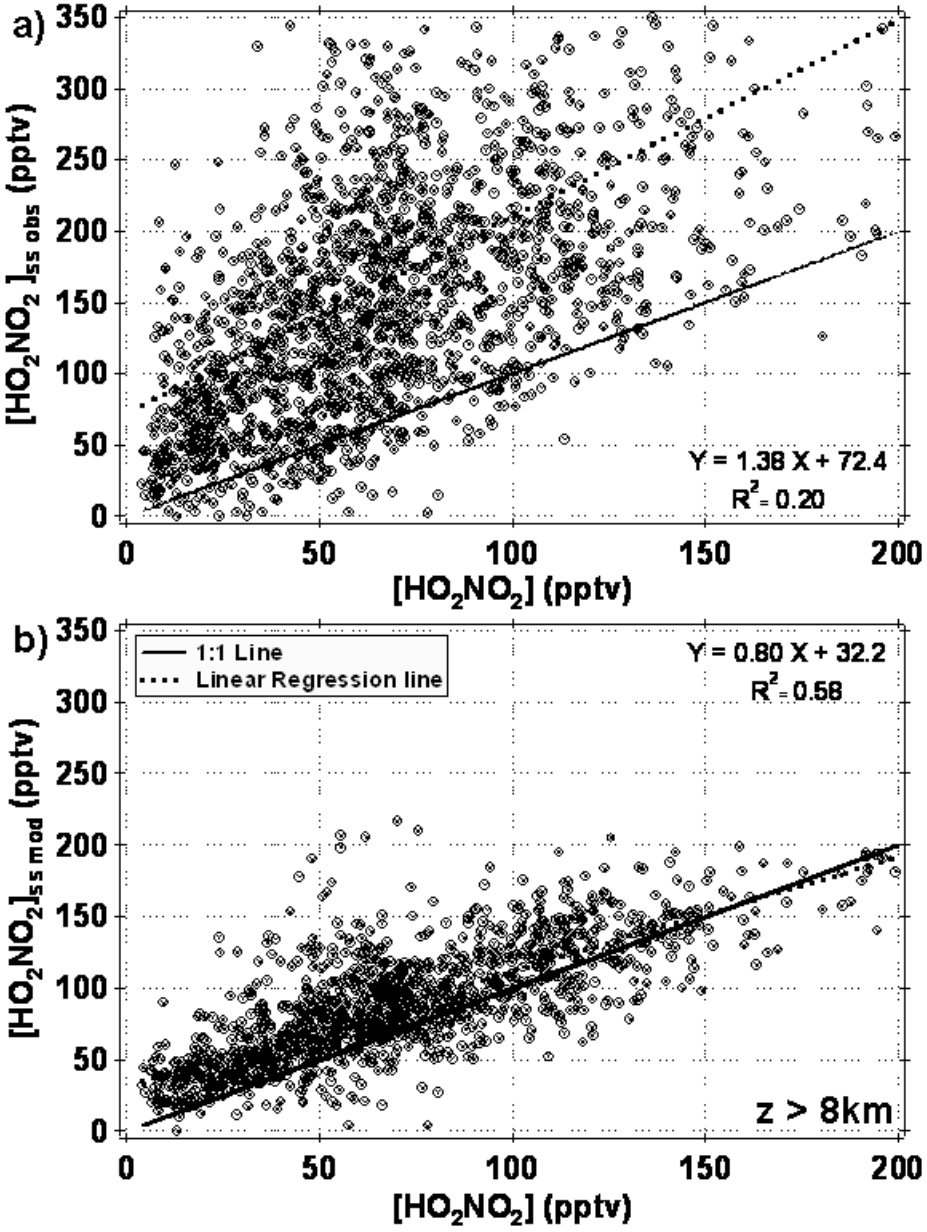

Figure 6. Scatters plots of upper troposphere (8-12 km) HO_2NO_2 steady state calculations versus observed HO_2NO_2. The calculations are based on observed (upper panel) and model (lower panel) HO_x.

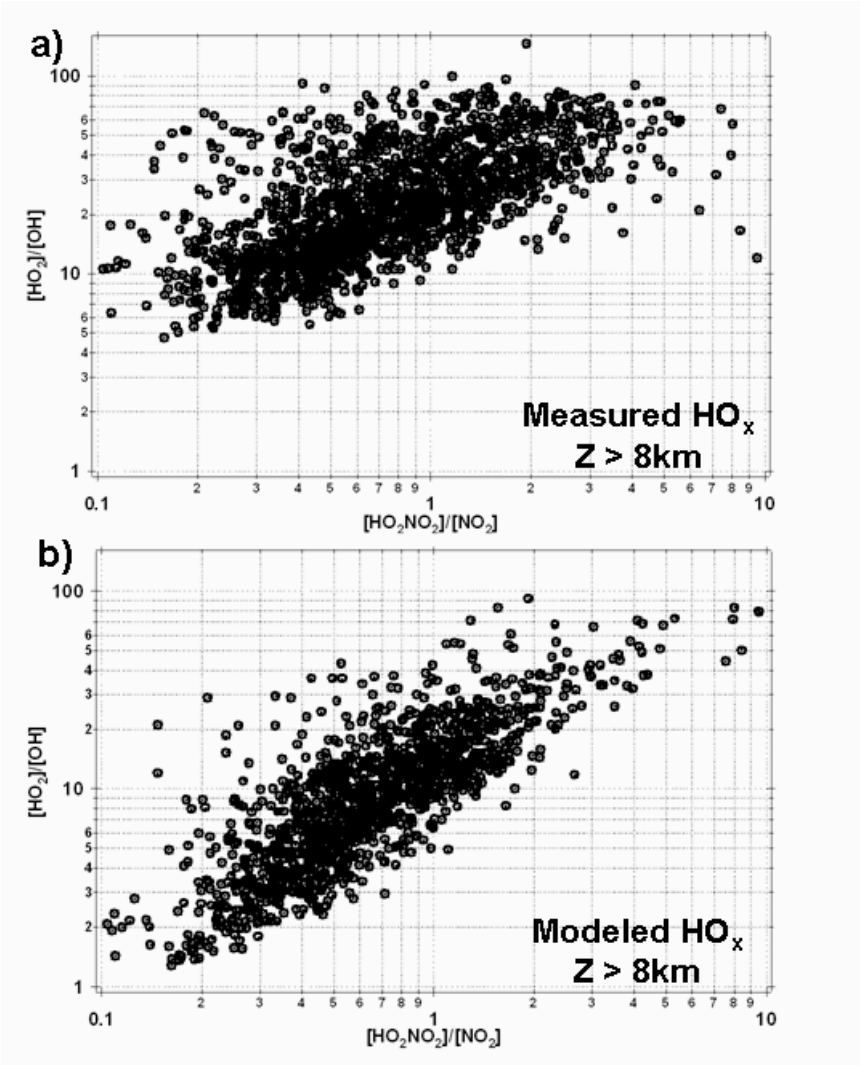

Figure 7. Correlation plot between $[HO_2NO_2]/[NO_2]$ and $[HO_2]/[OH]$(a) from observed HO_x b) from box model HO_x.

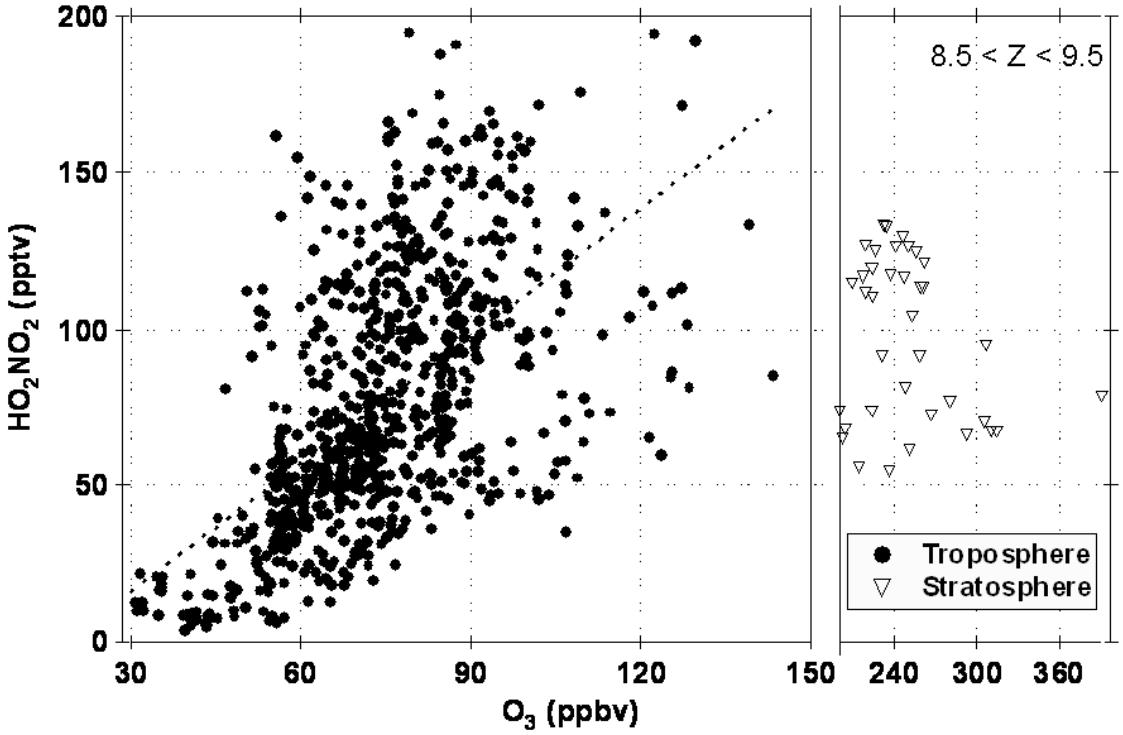

Figure 8. Scatter plot of HO_2NO_2 and O_3 in the altitude range of 8.5 to 9.5 km. Closed circles represent air primarily of tropospheric origin and open triangle represent air with significant stratospheric influence. Note the horizontal axis has a change in scale at 150 ppbv of ozone.

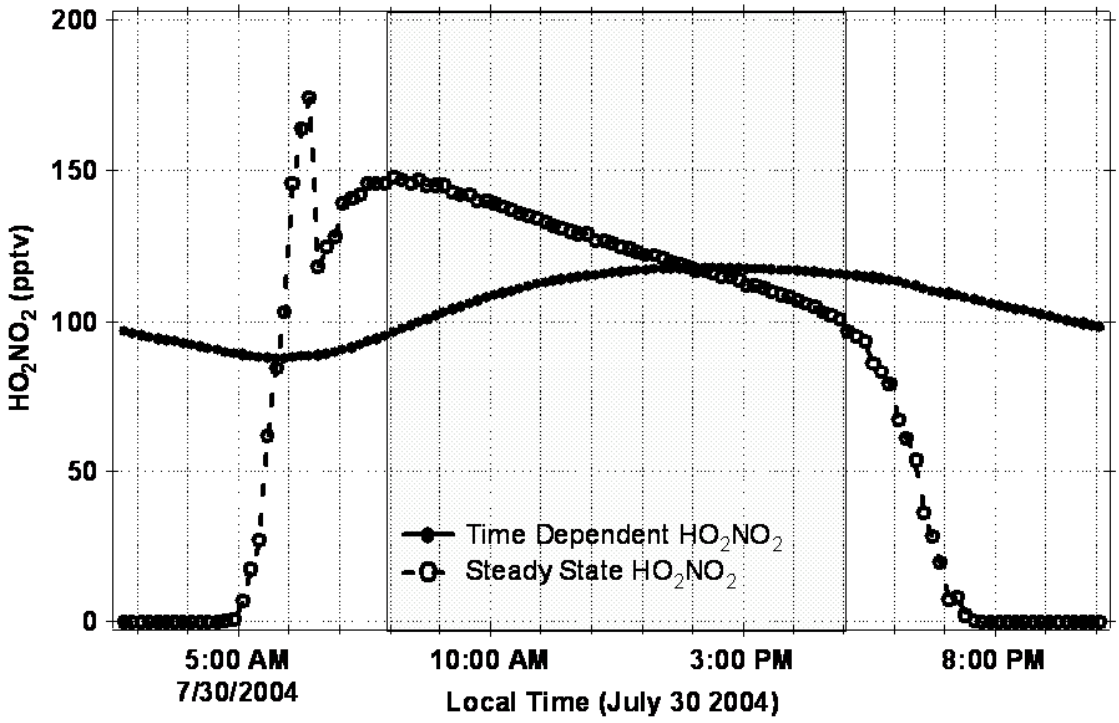

Figure 9. Temporal plot of HO_2NO_2 calculated using time-dependent (filled circle with solid line) and steady state HO_2NO_2 (open circle with dashed line) models. Shaded time zone is a typical flight time during the INTEX-NA from 8am to 5pm.

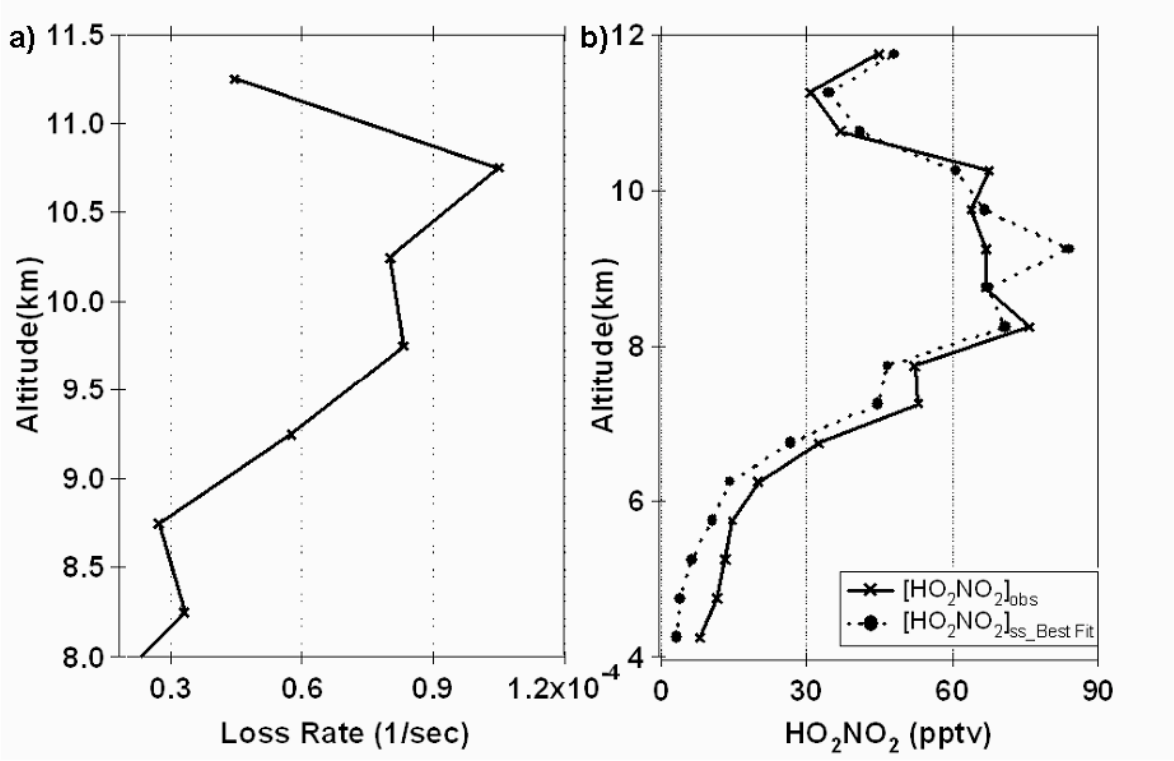

Figure 10. a) Altitude profile of the first order rate constant for the additional loss of HO_2NO_2 derived from measured HO_x. Vertical profile of observed ($[HO_2NO_2]_{obs}$) and predicted ($[HO_2NO_2]_{ss\_Best\ Fit}$). The predicted HO_2NO_2 is derived from a steady state analysis using observed OH levels and the model predicted ratio of $[HO_2]$ to $[OH]$.

Table 1. Summary of how chemical species are treated in the time-dependent model.

Category	Species
Constrained	O_3, CH_4, CO, CH_2O CH_3OOH, H_2O_2, $CH_3C(O)CH_3$, H_2O
Steady state	OH, HO_2, CHO , $O(^1D)$, CH_3O_2, $CH_3C(O)O_2$
Time dependent	NO, NO_2, HNO_3, HO_2NO_2, PAN, NO_3, N_2O_5

Table 2. Vertical distribution of observed HO_2NO_2 from 1 minute average data for INTEX-NA 2004

Altitude(km)	Median(pptv)	Average(pptv)	1σ(pptv)
4.25	8.0	12.3	15.9
4.75	11.4	15.8	20.7
5.25	13.4	31.3	62.7
5.75	15.6	20.5	15.5
6.25	20.4	25.6	18.4
6.75	32.2	38.9	24.0
7.25	53.7	59.2	32.4
7.75	51.9	61.5	39.3
8.25	78.2	77.5	39.6
8.75	66.8	75.1	39.9
9.25	67.8	75.8	41.4
9.75	62.6	65.0	32.5
10.25	63.0	66.1	29.7
10.75	38.7	44.1	25.2
11.25	34.1	41.0	23.8
11.75	46.0	46.8	10.7

Table 3. Parameters for actinic flux calculations using SBDART.

Local time	July 28th , Local noon
Latitude	38^{o}N
Surface type	Sand
Atmosphere profile	US 62
Boundary layer type	Rural

References

Bandy, A.R., D.C. Thornton, and A.R. Driedger III, Airborne measurements of sulfur dioxide, dimethyl sulfide, carbon disulfide, and carbonyl sulfide by isotope dilution gas chromatography/mass spectrometry, *Journal of Geophysical Research*, *98(D12)*, 23,432-23,433, 1993.

Brune, W.H., D. Tan, I.F. Faloona, L. Jaeglé, D.J. Jacob, B.G. Heikes, J. Snow, Y. Kondo, R. Shetter, G.W. Sachse, B. Anderson, G.L. Gregory, S. Vay, H.B. Singh, D.D. Davis, J.H. Crawfrord, and D.R. Blake, OH and HO_2 chemistry in the North Atlantic free troposphere, *Geophoysical Research Letter*, *25*, 1701-1704, 1999.

Christensen, L.E., M. Okumura, S.P. Sander, R.R. Friedl, C.E. Miller, and J.J. Sloan, Measurements of the rate constant of $HO_2+NO_2+N_2 \rightarrow HO_2NO_2+N_2$ using near-infrared wavelength-modulcation spectroscopy and UV-Visible absorption spectroscopy, *Journal of Physical Chemistry A*, *108*, 80-91, 2004.

Crawford, J., D. Davis, J. Olson, G. Chen, S. Liu, G. Gregory, J. Barrick, G. Sachse, S. Sandholm, B. Heikes, H. Singh, and D. Blake, Assessment of upper tropospheric HO_x sources over the tropical pacific based on NASA GTE/PEM data: Net effect on HO_x and other photochemical parameters, *Journal of Geophysical Research*, *104* (D13), 16,255-16,273, 1999.

Faloona, I., D. Tan, W.H. Brune, L. Jaeglé, D.J. Jacob, Y. Kondo, M. Koike, R. Chatfield, R. Pueschel, G. Ferry, G.W. Sachse, S. Vay, B. Anderson, J. Hannon, and H. Fuelberg, Observations of HO_x and its relationship with NOx in the upper troposphere during SONEX, *Journal of Geophysical Research*, *105* (D3), 3771-3783, 2000.

Gierczak, T., E. Jiménez, V. Riffault, J.B. Burkholder, and A.R. Ravishankara, Thermail decomposition of HO_2NO_2(Peroxynitric acid, PNA): Rate coefficient and determination of the Enthalpy of Formation, *Journal of physical Chemistry A*, *109*, 586-596, 2005.

Huey, L.G., D.R. Hanson, and C.J. Howard, Reactions of SF_6^- and I^- with atmospheric trace gases, *Journal of Physical Chemistry*, *99*, 5001-5008, 1995.

Huey, L.G., D.J. Tanner, D.L. Slusher, J.E. Dibb, R. Arimoto, G. Chen, D. Davis, M.P. Buhr, J.B. Nowak, R.L. Mauldin, F.L. Eisele, and E. Koschiuch, CIMS measurements of HNO_3 and SO_2 at South Pole during ISCAT 2000, *Atmospheric environment*, *38*, 5411-5421, 2004.

Jaeglé, L., D.J. Jacob, W.H. Brune, I. Faloona, D. Tan, B.G. Heikes, Y. Kondo, G.W. Sachse, B. Anderson, G.L. Gregory, H.B. Singh, R. Pueschel, G. Ferry, D.R. Blake, and R.E. Shetter, Photochemistry of HO_x in the upper troposphere at nothern midlatitude., *Journal of Geophysical Research*, *105* (3877-3892), 2000.

Jiménez, E., T. Gierczak, H. Stark, J. B. Burkholder, and A. R. Ravishankara, Reaction of OH with HO_2NO_2 (pernitirc acid): rate coefficient between 218 and 225 K and product yields at 298K, *Journal of Physical Chemistry A*, *108*, 1139-1149, 2004.

Li, Z., R.R. Friedl, S.B. Moore, and S.P. Sander, Interaction of peroxynitric acid with solid H_2O Ice, *Journal of Geophysical Research*, *101* (D3), 6759 - 6802, 1996.

Mathews, J., A. Sinha, and J.S. Francisco, The importance of weak absorption features in promoting tropospheric radical production, *Proceedings of the National Academy of Sciences of the United States of America, 102 (21)*: 7449-74452, 2005.

Murphy, J.G., J.A. Thornton, P.J. Wooldridge, D.A. Day, R.S. Rosen, C. Cantrell, R. Shetter, B. Lefer, and R.C. Cohen, Measurements of the sum of HO_2NO_2 and $CH_3O_2NO_2$ in the remote troposphere, *Atmospheric chemistry and physics discussions*, *3* (6), 5689-5710, 2003.

Niki, H., P.D. Marker, C.M. Savage, and L.P. Breitenbach, Fourier transform IR spectroscopy observation of pernitric acid formed via $HOO + NO_2 \rightarrow HOONO_2$, *Chemical physics letters*, *45* (3), 564-566, 1977.

OIson, J.R., J.H. Crawford, G. Chen, A. Fried, M.J. Evans, C.E. Jordan, S.T. Sandholm, D.D. Davis, B.E. Anderson, M.A. Avery, J.D. Barrick, D.R. Blake, W.H. Brune, F.L. Eisele, F. Flocke, H. Harder, D.J. Jacob, Y. Kondo, B.L. Lefer, M. Martinez, R.L. Mauldin, G.W. Sachse, R.E. Shetter, H.B. Singh, R.W. Talbot., and D. Tan, Testing fast photochemical theory during TRACE-P based on measurements of OH, HO_2 and CH_2O, *Journal of Geophysical Research*, *109*, D15S10,doi:10.1029/2003JD004278, 2004.

Ricchiazzi, P., S. Yang, C. Gautier, and D. Sowle, SBDART: A research and teaching software tool for plane-parallel radiative transfer in the earth's atmosphere, *Bulletin of the American Meteorology Society*, *79* (No. 10), 2101-2114, 1998.

Rinsland, C.P., M.R. Gunson, R.J. Salawitch, H.A. Michelsen, R. Zander, M.J. Newchurch, M.M. Abbas, M.C. Abrams, G.L. Manney, A.Y. Chang, F.W. Irion, A. Goldman, and E. Mahieu, ATMOS/ATLAS-3 measurements of stratospheric chlorine and reactive nitrogen partitioning inside and outside the November 1994 Antarctic vortex, *Geophoysical Research Letter*, *23* (17), 2365-2368, 1996.

Roehl, C.M., S.A. Nizkorodov, H. Zhang, G. Blake, and P.O. Wennberg, Photodissociation of peroxynitric acid in the Near-IR, *Journal of Physical Chemistry*, *106*, 3766-3772, 2002.

Rothman, L.S., D. Jacquemart, A. Barbe, D. Chris Benner, M. Birk, L.R. Brown, C.M. R., C.J. Charkerian, K. Chance, L.H. Coudert, V. Dana, V.M. Devi, J.-M. Flaud, R.R. Gamache, A. Goldman, J.-M. Hartmann, K.W. Jucks, A.G. Maki, J.-Y. Mandin, S.T. Massie, J. Orphal, A. Perrin, C.P. Rinsland, M.A.H. Smith, J. Tennyson, R.N. Tolchenov, R.A. Toth, J. Vander Auwera, P. Varanasi, and G.

Wagner, The HITRAN 2004 molecular spectroscopic database, *Journal of Quantitative Spectroscopy & Radiative Transfer*, *96*, 139 - 204, 2005.

Sander, S.P., A.R. Ravishankara, D.M. Golden, C.E. Kolb, M.J. Kurylo, R.E. Huie, V.L. Orkin, M.J. Molina, G.K. Moortgat, and B.J. Finlayson-Pitts, Chemical kinetics and photochemical data for use in atmospheric studieds, in *JPL PUb 02-25*, Pasadena, 2003.

Sen, B., G.C. Toon, G.B. Osterman, J.-F. Blavier, J.J. Margitan, R.J. Salawitch, and G.K. Yue, Measurements of reactive nitrogen in the stratosphere, *Journal of Geophysical Research*, *103* (D3), 3571-3585, 1998.

Shetter, R.E., and M. Müller, Photolysis frequency measurements using actinic flux spectroradiometry during the PEM-Tropics mission : Instrumentation description and some result, *Journal of Geophysical Research*, *104* (D5), 5647-5661, 1999.

Singh, H.B., A.M. Thompson, and H. Schlager, SONEX airborne mission and coordinated POLINAT-2 activity: overview and accomplishments, *Geophoysical Research Letter*, *26* (20), 3053-3056, 1999.

Sjostedt, S.J., D.J. Tanner, J.E. Dibb, M. Buhr, M. Warshawsky, D. Davis, G. Chen, R.L. Mauldin, F.L. Eisele, R. Arimoto, and L.G. Huey, Meaurement HO_2NO_2 and HNO_3 at South Pole during ANTCI 2003, in *American Geophysical Union Fall meeting*, pp. A24A-02, San Francisco, 2004.

Slusher, D.L., S.J. Pitteri, B.J. Haman, D.J. Tanner, and L.G. Huey, A chemical ionization technique for measurement of pernitric acid in the upper troposphere adn the polar boundary layer, *Geophoysical Research Letter*, *28*, 3875-3878, 2001.

Slusher, D.L., L.G. Huey, D.J. Tanner, G. Chen, D.D. Davis, M. Buhr, J.B. Nowak, F.L. Eisele, E. Kosciuch, R.L. Mauldin, B.L. Lefer, R.E. Shetter, and J.E. Dibb, Measurements of pernitric acid at the south pole during ISCAT 2000, *Geophoysical Research Letter*, *29* (21), 2011,doi:10.1029/2002GL015703, 2002.

Slusher, D.L., L.G. Huey, D.J. Tanner, F. Flocke, and J.M. Roberts, A thermal dissociation-chemical ionization mass spectrometry(TD-CIMS) technique for the simultaneous measurement of peroxyacyl nitrates and dinitrogen pentaoxide, *Journal of Geophysical Research*, *109* (D19315), doi:10.1029/2004JD004670, 2004.

Talbot., R.W., J.E. Dibb, E.M. Scheuer, Y. Kondo, M. Koike, H.B. Singh, L.B. Salas, Y. Fukui, J.O. Ballenthin, R.F. Meads, T.M. Miller, D.E. Hunton, A.A. Viggiano, D.R. Blake, N.J. Blake, E. Atlas, F. Flocke, D.J. Jacob, and L. Jaeglé, Reactive nitrogen budget during the NASA SONEX mission, *Geophoysical Research Letter*, *26* (20), 3057-3060, 1999.

Wennberg, P.O., R.J. Salawitch, D.J. Donaldson, T.F. Hanisco, E.J. Lanzendorf, K.K. Perkins, S.A. Lloyd, V. Vaida, R.S. Gao, E.J. Hintsa, R.C. Cohen, W.H. Swartz, T.L. Kusterer, and D.E. Anderson, Twilight

observations suggest unknown sources of HOx, *Geophoysical Research Letter*, *26*, 1373-1376, 1999.